Fusion Engineering and Design 202 (2024) 114397

Contents lists available at ScienceDirect

Fusion Engineering and Design

journal homepage: www.elsevier.com/locate/fusengdes

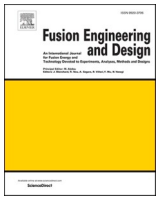

RELAP5-based thermal-hydraulic assessment of the STEAM facility for DEMO WCLL balance of plant analysis

Alessandra Vannoni [a], Pierdomenico Lorusso [b], Marica Eboli [c,*], Fabio Giannetti [a], Cristiano Ciurluini [a], Diego Jaramillo Sierra [d], Alessandro Del Nevo [c]

[a] DIAEE Department, Sapienza University of Rome, Rome 00186, Italy
[b] ENEA, Department of Fusion and Nuclear Safety Technology, Rome, Frascati I-00044, Italy
[c] ENEA, Department of Fusion and Nuclear Safety Technology, (BO), Camugnano 40032, Italy
[d] DENG Department, Politecnico di Milano, Milan 20156, Italy

ARTICLE INFO

Keywords:
STEAM
Balance of plant
Demo
Water technology
Experimental facility
OTSG mock-up

ABSTRACT

DEMO power station aims to demonstrate the generation of hundred MWs of electrical power from fusion reactions, then transmitted from the Tokamak reactor to the grid through the Balance of Plant (BoP). The design approach for the Water Cooled Lithium Lead (WCLL) Breeding Blanket (BB) Primary Heat Transfer Systems (PHTSs) leverages nuclear industry expertise but faces challenges due to DEMO pulsed operation and low-load periods. To assess the feasibility of these components, ENEA Experimental Engineering Division at Brasimone R.C. is designing STEAM, a facility investigating water technologies applied to the DEMO BB and BoP systems and components. STEAM is mainly composed of a primary system reproducing the DEMO WCLL BB PHTS thermodynamic conditions (15.5 MPa, 328–295 °C) and a secondary two-phase (liquid/steam) loop reproducing the DEMO power conversion system conditions (6.4 MPa, 238–300 °C). Experimental validation will reproduce steady-state and transient operation under DEMO-relevant conditions, including dedicated tests on the DEMO once through steam generator mock-up.

STEAM objectives and description are presented in this paper, together with the RELAP5/Mod3.3 nodalization of the facility. The latter is used to, thermal-hydraulically characterize the facility behaviour. The outcomes of the steady-state qualification supported the optimization of the system layout appraising the performances of key components under the specified operating conditions.

1. Introduction

Nuclear fusion constitutes a form of energy generation that harnesses the fusion of light atomic nuclei to produce a substantial amount of energy. In contrast to nuclear fission, the process underlying current nuclear power plants, in nuclear fusion light nuclei, such as hydrogen isotopes, react to form helium, releasing considerable energy in the process. Among its advantages, fusion offers a highly efficient and potentially inexhaustible energy source, utilizing abundant light isotopes like deuterium. Instead, tritium, a crucial component for some fusion reactions, is scarce in nature because it is radioactive, and it is characterized by a relatively short half-life of 12.32 years. It can, though, be generated *in-situ* through the interaction of neutrons with lithium. However, the practical implementation of fusion is complex, requiring extremely high temperatures and pressures to maintain the plasma in a reactive state. Some of the primary challenges include managing extreme conditions, designing materials capable of withstanding the harsh environment and achieving sustained, controlled reactions. Despite these hurdles, the promise of clean, abundant energy motivates ongoing international efforts to unlock the full potential of nuclear fusion.

In the pursuit of advancing fusion energy as a sustainable and clean power source, international efforts have converged on the development and operation of state-of-the-art experimental facilities and fusion reactors. Among these, the EUropean DEMOnstration reactor (EU-DEMO) [1] exemplifies a fundamental milestone, relying on innovative approaches for managing the intense thermal and neutronic loads generated by the plasma. One of the key reactor components is the Breeding Blanket (BB), accomplishing several functions, such as cooling device, tritium breeder, and neutron shield. Two BB concepts [2] are currently

* Corresponding author.
E-mail address: marica.eboli@enea.it (M. Eboli).

https://doi.org/10.1016/j.fusengdes.2024.114397
Received 26 January 2024; Received in revised form 1 March 2024; Accepted 25 March 2024
Available online 27 March 2024

under investigation: the Water-Cooled Lithium-Lead (WCLL) and the Helium-Cooled Pebble Bed (HCPB) [3], relying on different coolants (i.e., water and helium) for managing the heat generated within the component by the nuclear reactions. Notably, the use of pressurized water as a coolant for the exposed walls represents a critical engineering solution in the WCLL concept, ensuring both efficient heat dissipation and radiation shielding. This approach is not unique to EU-DEMO; several international projects are currently underway, showcasing a global commitment to harnessing fusion power.

One notable endeavor is the ITER (International Thermonuclear Experimental Reactor) project [4], a collaborative effort involving 35 countries. ITER, based in France, aims to demonstrate the feasibility of large-scale fusion power and is equipped with advanced water-cooling systems to withstand the extreme conditions generated by the fusion process. ITER will conduct tests on different BB concepts in the form of Test Blanket Modules (TBMs) [5]. In particular, the WCLL TBM will test the DEMO WCLL BB in an integrated fusion environment for the first time. This blanket mock-up will be actively cooled by the Water Cooling System (WCS), with water injected at 15.5 MPa and 295 °C, removing up to nearly 750 kW of thermal power while maintaining the structural integrity of the reactor [6].

Similarly, the Chinese Fusion Engineering Test Reactor (CFETR) [7,8] is poised to become a key player in the fusion research landscape. Planned to be the world's largest tokamak, CFETR also integrates water-cooled systems into its design, reflecting a shared emphasis on the efficacy of pressurized water as a coolant. CFETR employs pressurized water at conditions of around 155 bar and 285–325 °C, circulating through dedicated cooling loops to manage the thermal loads induced by the plasma.

KSTAR (Korea Superconducting Tokamak Advanced Research) [9,10] from South Korea advances fusion research with its superconducting tokamak, incorporating water-cooling systems operating at approximately 160 bar and 320 °C. The pressurized water serves a critical role in dissipating heat from the plasma-exposed surfaces.

These international initiatives underscore the significance of water-cooled systems in shaping the future of fusion energy. As the global community collaborates to overcome the scientific and engineering challenges associated with these ambitious projects, the research presented here not only addresses the specific challenges of water-cooled systems but also contributes valuable insights to the broader international pursuit of harnessing fusion as a safe and reliable energy source.

With this aim, the main European countries have gathered their research efforts by funding EUROfusion, a European consortium for nuclear fusion development [11]. ENEA (Italian National Agency for New Technologies, Energy and Sustainable Economic Development) collaborates with EUROfusion to support the development and the design of systems and components suitable for nuclear fusion technologies and nuclear R&D. ENEA Brasimone Research Centre [12] has recently undertaken a research initiative to design and realize a multi-purpose experimental infrastructure, named W-HYDRA [13,14]. This facility is conceived to investigate the application of water and lithium-lead technologies to the DEMO BB and Balance of Plant (BoP) systems [15].

Within the W-HYDRA infrastructure, STEAM [16,17] serves as a water facility specifically designed for the experimental exploration of the DEMO BoP, with a primary focus on the STEAM Generator (SG) of the WCLL BB Primary Heat Transfer System (PHTS) [18,19]. It primarily consists of two loops that are hydraulically independent but thermally coupled through a Test Section (TS, i.e., the SG) [20], designed for a maximum power of 3.1 MW. The experimental validation of the DEMO BoP water coolant systems will involve steady-state tests, transient scenarios, and specific tests aimed at demonstrating the SG capability to accommodate the DEMO power phases and the corresponding transitions. This is crucial because the SG envisaged for DEMO is expected to operate in a pulsed regime since currently, no systems are capable of indefinitely sustaining the current that generates the plasma. The resulting plasma-generated thermal power differs from the conventional continuous power production characteristic of a fission reactor for which the Once Through Steam Generator (OTSG) [22] has been designed [21]. Thus, the component requires reliable control procedures to be defined and tested.

Table 1
STEAM main data.

Parameter Label	Unit	Value	Parameter Description
Primary side			
P	MW	3.1	Power delivered by TS from primary to secondary side
$p_{H2O,1}$	MPa	15.5	H_2O pressure in the primary side
$T_{H2O,in,1}$	°C	328.0	H_2O temperature at the TS inlet
$T_{H2O,out,1}$	°C	295.0	H_2O temperature at the TS outlet
$\Gamma_{H2O,1}$	kg/s	16.05	H_2O mass flow rate
Secondary side			
$p_{H2O,2,\ upstream\ lam.}$	MPa	6.4	H_2O pressure upstream the lamination
$p_{H2O,2,\ downstream\ lam.}$	MPa	2.5	H_2O pressure downstream the lamination
$T_{H2O,in,2}$	°C	238.0	H_2O temperature at TS inlet
$T_{H2O,out,2}$	°C	≥300.0	H_2O temperature at TS outlet
$\Gamma_{H2O,2}$	kg/s	1.63	H_2O mass flow rate

In this paper, the STEAM facility layout is presented, providing details on the main components and the operational parameters. Thermal-Hydraulic (T/H) analyses of STEAM were carried out using RELAP5/Mod3.3 [23] code. Steady-state results are collected and discussed focusing on the assessment of the performances of the Air Cooler modules (ACs), adopted as the final heat sink for the facility. The feedbacks of the computational analyses are crucial for refining the control logics to be implemented and optimizing the facility configuration.

2. STEAM facility outlines and description

The objective of the STEAM facility to experimentally characterize and validate the OTSG component in fusion applications arises from the distinct operational conditions of fission and fusion reactors. Specifically, fission reactors, along with their Balance of Plant (BoP), are designed to keep the power at an approximately constant level close to the maximum capability of the system. The Balance of Plant consists in the collection of auxiliary components and systems necessary for the overall operation of a reactor or power plant excluding the primary equipment responsible for power generation, therefore applies to both fission and fusion reactors. In a nuclear power plant, the BoP plays a critical role in managing various aspects of plant operation, including cooling systems, electrical distribution, control and instrumentation, safety systems, and environmental management. In the context of the DEMO fusion reactor with WCLL BB, the BoP shares similarities with that of a fission reactor in terms of constituent components (pressurizer, pumps, heat exchangers, cooling loops…). However, it significantly diverges in operational conditions due to inherent differences in reactor technology. Consequently, while the fundamental components may bear resemblance, the operational environments pose distinct challenges and requirements.

In fusion reactors, the power generated by the plasma is discontinuous, fluctuating from 100 % (pulse) to 1 % (dwell) and vice versa [24]. The DEMO WCLL BB BoP design assumptions based on a direct coupling [25] currently envisages a power cycle consisting of 2-hour pulses followed by 10 min of dwell at decay power [26,27]. Due to these specific operational characteristics, the qualification of the use of OTSG and, more in general, of the BoP in fission applications cannot be directly extended to fusion scenarios but requires validation through experimental facilities.

To address this challenge, STEAM will function as an experimental facility to assess the behavior of the OTSG not only during rapid power variations associated with the plasma but also at power levels corresponding to the dwell phase. This comprehensive testing approach is

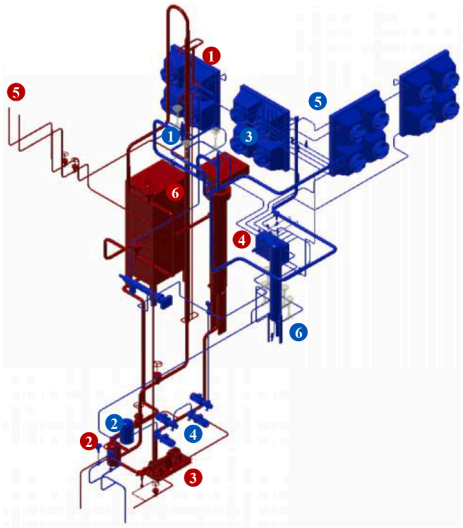

Fig. 1. 3D view of STEAM primary (red) and secondary system (blue). Reference of numbers in figure are reported along the text.

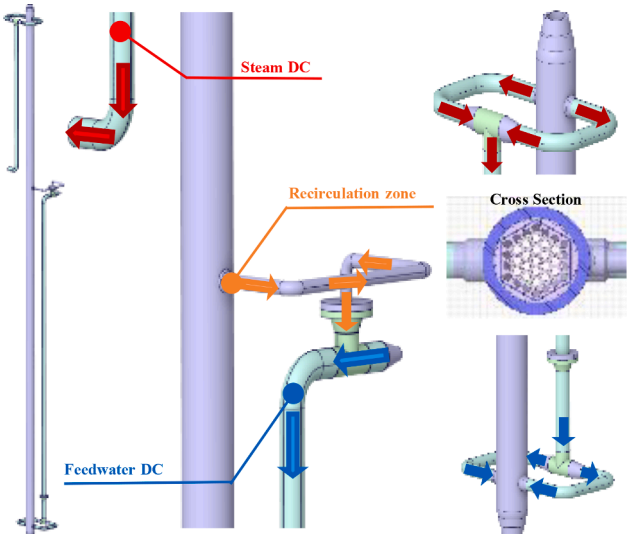

Fig. 2. STEAM OTSG mock-up.

essential to validate the suitability and performances of the OTSG component in the dynamic and varied conditions typical of fusion applications.

The main thermal-hydraulic parameters of the STEAM facility are collected in Table 1.

STEAM primary loop will allow the experimental characterization of two test sections: the DEMO STEAM generator mock-up (i.e., Test Section 1, TS 1) and the WCLL manifold mock-up (i.e., Test Section 2, TS2). The TS2 [28] is a scaled-down test section representative of an Outboard segment manifold of the WCLL Breeding Blanket for DEMO. It aims to experimentally confirm the flow repartition computed in the different breeding units on the full-scale manifold, validating at the same time the computational tools used for the design and analysis.

Referring to the 3D CAD representation of the STEAM facility in Fig. 1, the primary loop (highlighted in red) comprises essential components crucial for experimental investigations. In the OTSG mock-up (1), pivotal for assessing performances under fusion-relevant conditions, primary fluid cools down flowing downwards tube side from 328 °C to 295 °C, exchanging 3.1 MW with the shell-side fluid. The OTSG detailed CAD is reported in Fig. 2. Sequentially, the fluid pathway

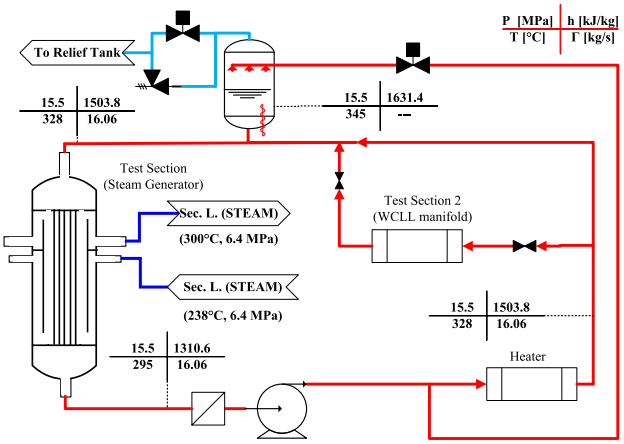

Fig. 3. Conceptual scheme of the STEAM PS.

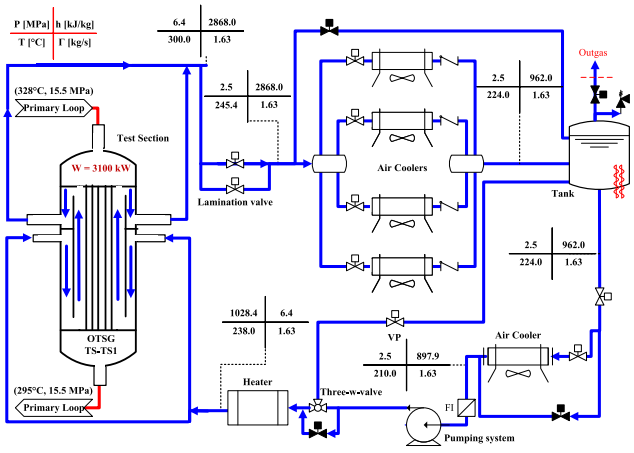

Fig. 4. Conceptual scheme of the STEAM SS.

encompasses a filter (2) to ensure fluid purity, followed by a high-efficiency pump (3) to provide the primary forced circulation. An electrical heater (4) of 3.25 MW of design power with U-shaped heating rods arranged in a triangular pitch pattern restores fluid thermal energy, ensuring the required thermal-hydraulic conditions at the OTSG inlet. Additionally, a pressurizer (5, not depicted in Fig. 1) is employed to maintain the reference circuit pressure, crucial for system integrity. Test Section 2 (6) is placed in series with the OTSG and is conceived to operate at constant temperature, without a power supply (except the amount required to compensate the loop heat losses). In the STEAM configuration, the manifold test section is by-passed. The primary loop conceptual scheme showing the Primary Side (PS) fluid path is illustrated in Fig. 3.

The secondary loop (depicted in blue in Fig. 1) is composed of several key components crucial for its operation. The OTSG (1) serves as heat source for this loop: fluid enters the downcomer and is pre-heated by superheated STEAM spilled by the tube bundle, reaches the lower tube sheet, and inverts its direction. It heats up flowing upwards shell-side in the riser and the produced superheated STEAM enters the steam-downcomer as soon as the upper tube-sheet is reached. To effectively regulate the OTSG outlet pressure, a lamination valve (3) is placed on the STEAM line. Within the component, the Secondary Side (SS) fluid undergoes an isenthalpic process. This process involves reducing the pressure from 6.4 MPa to 2.5 MPa, decoupling the STEAM generator from the rest of the loop and avoiding propagation of eventual instability towards the test section. Since no turbine is envisaged, air coolers (5)

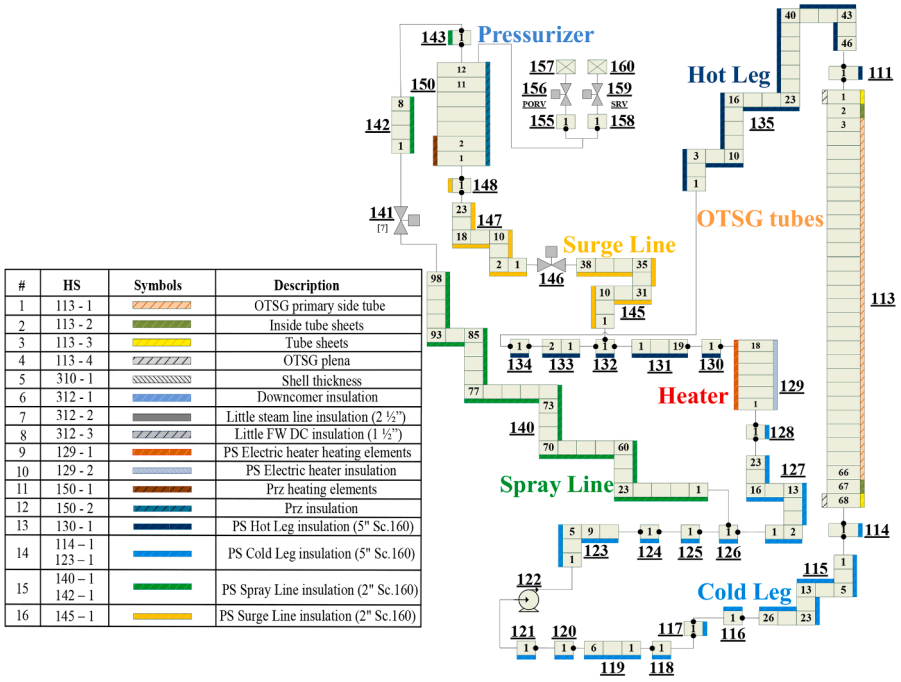

#	HS	Symbols	Description
1	113 - 1		OTSG primary side tube
2	113 - 2		Inside tube sheets
3	113 - 3		Tube sheets
4	113 - 4		OTSG plena
5	310 - 1		Shell thickness
6	312 - 1		Downcomer insulation
7	312 - 2		Little steam line insulation (2 ½")
8	312 - 3		Little FW DC insulation (1 ½")
9	129 - 1		PS Electric heater heating elements
10	129 - 2		PS Electric heater insulation
11	150 - 1		Prz heating elements
12	150 - 2		Prz insulation
13	130 - 1		PS Hot Leg insulation (5" Sc.160)
14	114 – 1 123 – 1		PS Cold Leg insulation (5" Sc.160)
15	140 – 1 142 – 1		PS Spray Line insulation (2" Sc.160)
16	145 – 1		PS Surge Line insulation (2" Sc.160)

Fig. 5. STEAM PS RELAP5/Mod3.3 nodalization.

play a crucial role in heat dissipation, ensuring optimal thermal management within the loop. Divided into two distinct components, the air coolers are designed to handle specific aspects of fluid conditioning. The first component, referred to as A.C.1, is divided into four modules designed to handle one-fourth of the total mass flow rate, thus facilitating the power operation of the facility. It is primarily responsible for de-superheating and condensing the STEAM, which is then collected and stored in the condensate tank (6). The second component, A.C.2, focuses on sub-cooling the fluid stored in the tank, completing the thermal conditioning process. A filter (2) ensures the required fluid quality and a pump (4) drives fluid circulation within the loop towards the OTSG. The secondary loop conceptual scheme showing the SS fluid path is

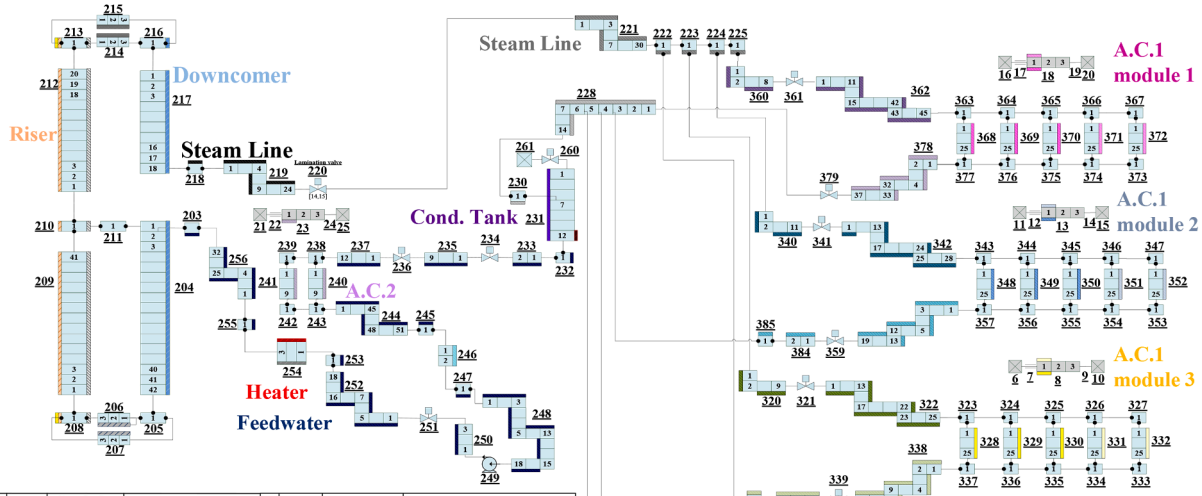

#	HS	Symbols	Description	#	HS	Symbols	Description
1	310-1		Shell thickness	19	371-1		A.C.4 tubes 34 to 55
2	312-1		Downcomer insulation	20	378-1		Small Cond. Line 4
3	312-2		Little steam line ins.	21	113-1		OTSG primary side tube
4	312-3		Little FW DC ins.	22	113-2		Inside tube sheets
5	300-1		Small Steam Line 1	23	113-3		Tube sheets
6	308-1		A.C.1 tubes 1 to 33	24	113-4		OTSG plena
7	311-1		A.C.1 tubes 34 to 55	25	218-1		Main Steam Line (3 ½")
8	318-1		Small Cond. Line 1	26	221-1		Main Steam Line (5")
9	320-1		Small Steam Line 2	27	228-1		Main Condensation Line
10	328-1		A.C.2 tubes 1 to 33	28	231-1		Condensate Tank insulation
11	331-1		A.C.2 tubes 34 to 55	29	231-2		Condensate Tank heaters
12	338-1		Small Cond. Line 2		232-1		
13	340-1		Small Steam Line 3		244-1		
14	348-1		A.C.3 tubes 1 to 33	30	247-1		Feedwater (1 ½") insulation
15	351-1		A.C.3 tubes 34 to 55		250-1		
16	358-1		Small Cond. Line 3		255-1		
17	360-1		Small Steam Line 4	31	140-1		A.C.5 tubes
18	368-1		A.C.4 tubes 1 to 33	32	246-1		Filter insulation

Fig. 6. STEAM SS RELAP5/Mod3.3 nodalization.

illustrated in Fig. 4.

A "power to volume" approach was adopted to achieve an OTSG mock-up design, keeping the full-length scale of the Breeding Zone (BZ) OTSG [18,29]. This methodology involves analyzing the relationship between the power generated or transferred within a system and the volume occupied by the component within that system to scale volumes and power with the same factor. Specifically, assuming the power/tube ratio to be constant, a scaling factor was calculated as the ratio of the STEAM and the OTSG BZ power. The resulting power factor was assumed to scale both the tube numbers and the volumes by multiplying the BZ tube number and flow areas by it, without modifying components lengths nor relative positions. With respect to the reference model, no distortions were introduced in the PS fluid path. Regarding the secondary side, geometrical constraints led to the replacement of the annular downcomer with an external pipe, thermally decoupled from the riser but designed to preserve the OTSG main features (i.e., the recirculation zone, the concentrated loss coefficient associated with the orifice plate). For further details see [20].

3. RELAP5 system T/H analysis

3.1. RELAP5 modeling activity

The RELAP5/Mod3.3 modeling activity allowed the realization of a mono-dimensional nodalization of the facility. The 1-D model of the primary system is depicted in Fig. 5. The OTSG plena and tubes are simulated by pipe 113, while branches 111 and 114 reproduce the inlet and outlet nozzles. The cold leg is replicated by components from 115 to 128 (where branch 117 is the filter and component 122 is the pump), while pipe 129 is the main electrical heater. Components from 130 to 135 model the hot leg, while the pressurizer system, composed of the surge line, the spray line, the main tank, and the valve relief system located at the component top, is realized with components from 140 to 160.

Fig. 6 shows the nodalization of the STEAM secondary loop. The OTSG is modeled by components from 203 to 218. In particular, components from 203 to 205 simulates the FeedWater (FW) downcomer, pipes 206 and 207 realize the tubes connecting riser and external downcomer, components from 208 to 213 stand for the riser, pipes 214 and 215 reproduce the tubes connecting riser and downcomer, while components from 214 to 218 represent the STEAM downcomer. The STEAM line is realized with branches and pipes from 218 to 225, where component 220 is the lamination valve. The A.C.1 four modules nodalization is symmetric, although minor differences exist in the length of the pipes reaching each module due to spatial constraints. It was realized using numbers from 300 to 385. In the following the nodalization scheme associated with each component is explained in detail by using X, Y, and Z, whose values are: X=0,2,4,6 (one for each A.C.), Y=1,3,5,7 (one for each A.C.) and Z=0,1,2,3,4,5 (used to identify the different tube groups belonging to each A.C.). The adopted hydrodynamic components are:

- Pipe 3X0 is the small STEAM line upstream the air cooler regulation and interception valve;
- Valve 3X1 is the regulation and interception valve;
- Pipe 3X2 represents the part of the small STEAM line that connects the valve with the air cooler;
- Branches 3X3, 3X4, 3X5, 3X6 and 3X7 realize the inlet header (1 ¼" Sch. STD);
- Pipes 3X8, 3X9, 3Y0, 3Y1, and 3Y2 are the air cooler active vertical tubes: each module is modeled with five pipes and each pipe collapses the flow area of 11 tubes for a total of 55 tubes for module;
- Branches 3Y3, 3Y4, 3Y5, 3Y6, and 3Y7 realize the outlet headers (1 ¼" Sch. STD), allowing the reaching of a uniform temperature at the component outlet;
- Pipes 3Y8 and 38Z represent the small condensation line (1 ¼" Sch. STD);
- Valve 3Y9 is the interception line installed on the small condensation line (1 ¼" Sch. STD).
- Referring to the A.C. air (secondary) side, the following components are adopted:
- Time-dependent volumes 1, 6, 11, and 16 impose the air inlet temperature;
- Time-dependent junctions 2, 7, 12, and 17 fix the inlet air mass flow;
- Pipes 3, 8, 13, and 18 stand for the A.C. shell side;
- Single junctions 4, 9, 14, and 19 allow the connection to the outlet time-dependent volumes;
- Time-dependent volumes 5, 10, 15, and 20 impose the air outlet pressure.

It must be noted that the nodalization numbers reported above are referred to all four components. Considering again the STEAM water secondary loop, the main condensation line is simulated by pipe 228 and branch 230, pipe 231 models the condensate tank and valve 260, and volume 261 realize its depressurization system. The feedwater goes from component 232 to 256, comprehending the subcooling air cooler (from 238 to 243), the pump (component 249), and the electrical heater (pipe 254).

The steady state of the STEAM experimental setup was achieved by equipping the nodalization with control systems monitoring to convergence of the main parameters (see Table 1):

- PS pump velocity is adjusted to maintain the nominal mass flow rate;
- PS electrical heater power is regulated to obtain the required temperature at the OTSG PS inlet;
- PS pressurizer is equipped with electrical heaters, a spray line, and relief valves, all operated to keep the corresponding system pressure;
- SS pump velocity is regulated to keep the nominal OTSG PS outlet temperature. Indeed, such temperature is the direct result of the power exchanged between primary and secondary loop, which in turn depends on the feedwater mass flow;
- SS electrical heater power is varied to obtain the required temperature at the OTSG SS inlet;
- SS A.C.2 air velocity is regulated to fix the nominal temperature at the SS pump suction section (210 °C);
- Condensate tank is equipped with electrical heaters and a relief valve, both operated to keep the corresponding system pressure.

3.2. RELAP5 models and correlations

Being the STEAM secondary side a two-phase loop, the main phenomena involved in the normal operation are boiling and condensation. Their numerical prediction is important for the correct evaluation of the performances of the main components (i.e., STEAM Generator and Air Coolers). The RELAP5 simulation of such conditions is based on the use of experimental correlations implemented in the code.

Several Heat Transfer modes (HTMs) are coded. Each one corresponds to a regime being used to transfer heat between the fluid and the solid surface. The HTM selection is performed depending on the fluid and wall properties characterizing the considered heat transfer problem.

In the SG secondary side, water experiences the phase transition from saturated liquid (at the bottom) up to superheated STEAM (at the top). To evaluate the corresponding Heat Transfer Coefficient (HTC), RELAP5/Mod3.3 adopts different correlations according to the predicted HTM, [30]. When the fluid is subcooled and the wall temperature (T_{wall}) is below the saturation temperature at the fluid total pressure (T_{sat} (P_{total})), single-phase liquid convection HTM is predicted by the code. For it, the adopted HTC correlation is Dittus-Boelter (D-B), [31]. In case the fluid flows outside a tube bundle, the enhanced turbulence induced by the latter is taken into consideration by multiplying the D-B HTC with the turbulent flow corrective factor developed by Inayatov,

Table 2
Steady-state characterization of RELAP5/Mod3.3 STEAM nodalization.

Parameter	Unit	Ref. Data	R5	Error[a]
Power				
PS e-heater	MW	3.1	3.1	0.0 %
TS	MW	3.1	3.1	0.0 %
PS pressurizer heaters	kW	12[b]	3.27	–
SS A.C.1	MW	3.108	3.25	+4.6 %
SS A.C.2	kW	104.0	67.1	−55 %
SS heater	kW	173.0	193.8	+12 %
SS tank heaters	kW	25[b]	13.2	–
SS additional source	kW	–	226.17	–
Mass Flow				
PS	kg/s	16.05	16.05	0.0 %
SS	kg/s	1.69	1.64	−3.0 %
Temperature				
PS OTSG inlet/PS e-heater outlet	°C	328.0	328.0	0° C
PS OTSG outlet/PS e-heater inlet	°C	295.0	295.0	0 °C
SS OTSG inlet/SS e-heater outlet	°C	238.0	237.8	−0.2° C
SS OTSG outlet	°C	300.0	314.7	+14.7° C
SS upstream A.C.1 (average between the four modules)	°C	245.4	264.6[c]	+19.2 °C
SS tank	°C	224.0	219.0	−5.0 °C
SS A.C.2 outlet	°C	210.0	210.0	0° C

[a] Error [%] = (R5–Ref)/Ref.
[b] Nominal installed power.
[c] Temperature that corresponds to the computed SG outlet enthalpy at 25 bar.

[32]. This coefficient is based on the tube pitch-to-tube diameter ratio, i.e., p/OD.

When the T_{wall} becomes higher than the T_{sat} (P_{total}), the fluid begins to boil on the tube outer surface. The latter remains wetted while small bubbles rapidly form and break away from it. Thanks to the turbulence due to the bubble formation, this heat transfer mode, called Nucleate Boiling, ensures a high heat transfer coefficient. It can be distinguished in Subcooled and Saturated Nucleate Boiling, according to the fluid bulk temperature, which can be less or equal to T_{sat} (P_{total}). In both cases, the Chen correlation, [33], is used by RELAP5/Mod3.3 to evaluate the wall-to-fluid heat transfer coefficient.

The process of nucleate and forced convective boiling persists until sufficient water is vaporized, replacing the liquid layer on the outer surface of the tube with a STEAM blanket, hindering heat transfer due to the insulating effect of the vapor layer. This phenomenon is called dry-out and causes a sharp reduction in the heat transfer efficiency, and a significant increase of the T_{wall}, primarily due to diminished contact between the heated surface and the fluid. This phenomenon is of critical importance in thermal systems as it marks a transition from efficient heat transfer to less effective modes. The corresponding heat flux value is named Critical Heat Flux (CHF). When CHF occurs, the heat transfer mechanism shifts to convection through the STEAM and evaporation of entrained liquid droplets in the saturated core. This less efficient HTM is referred to as Film Boiling. To evaluate the CHF (i.e., the dry-out occurrence), RELAP5/Mod3.3 uses the 1986 Groeneveld Look-Up Tables (LUT, [34]). It is important to note that the code does not differentiate between burnout and dry-out, leveraging on the fact that the effects are analogous. In the post-dry-out region, the system code compares the HTCs evaluated with two different correlations: the Chen transition boiling model, [35], and the Bromley film boiling model corrected by Sudo, [36,37]. Then, the higher is adopted.

Finally, when the fluid void fraction (α_g) exceeds 0.999, the HTM predicted by the code is single-phase vapor convection. The corresponding HTC is evaluated as for the single-phase liquid convection but by considering the STEAM properties instead of the liquid ones.

The condensation problem is called when the wall temperature is below the saturation temperature based on the partial pressure of STEAM, the void fraction is above 0.1 and the noncondensable mass quality is lower than 0.999. Thus, when the gas phase is relevant and a significant fraction of it is constituted by the fluid STEAM phase (and not from transported noncondensables).

Regarding condensation, the default option in RELAP5 is the maximum of the Nusselt [38] (laminar) and Shah [39,40] (turbulent) correlations with a diffusion calculation when non-condensable gases are present.

$$h_c = \max(h_{Nusselt},\ h_{Shah}) \tag{1}$$

$$h_{Nusselt} = \frac{k_f}{\left(\frac{3\mu_f \Gamma}{g\rho_f \Delta\rho}\right)^{\frac{1}{3}}} \tag{2}$$

$$h_{Shah} = h_l(1-X)^{0.8}\left(1+\frac{3.8}{\left(\left(\frac{1}{X}-1\right)^{0.8} P_{red}^{0.4}\right)^{0.95}}\right) \tag{3}$$

Where h_l is the Dittus Boelter heat transfer coefficient assuming all fluid is liquid.

3.3. RELAP5 steady-state characterization of the STEAM facility

RELAP5/Mod3.3 system code was adopted to simulate the thermal-hydraulic behavior of the whole facility, thermally coupling the primary and secondary loops. Steady-state results of Table 2 show that the secondary side vapor outlet temperature exceeds the nominal value. This discrepancy is a direct consequence of the SG sizing obtained by adopting a scaling procedure from the DEMO BB PHTS OTSG at Beginning of Life (BoL) conditions. This approach involved selecting a number of tubes to ensure that the facility can meet its power requirements even under less-than-optimal conditions (such as End of Life, EoL, scenarios marked by performance degradation due to tube fouling and plugging). Thus, if EoL operations were simulated, the SG outlet temperature would be aligned with the design one reported in Table 2. Instead, at BoL, being the SG heat transfer capability enhanced by the absence of the tube fouling and plugging, the vapor outlet temperature also results increased. This produces a higher enthalpy at the suction of the lamination valve, causing the expansion through the valve to also occur at a higher enthalpy. Nonetheless, in the volume downstream the valve that causes the flow to choke, RELAP5 code is not able to properly reproduce the isenthalpic process, as theoretically expected. To address this problem from a simulation point of view, a source term was introduced at the valve outlet. It provides the secondary water with the needed power to restore the enthalpy content associated with the STEAM generator outlet section. This additional term is indicated in Table 2, labeled as 'SS additional source'. Consequently, the temperature mismatch at the SG outlet also produces the one at the valve outlet (see in Table 2 the row labeled 'SS upstream A.C.1'). Indeed, the reference enthalpy for the lamination process is aligned with the SG outlet one, which is higher than the nominal value (same STEAM line pressure but higher outlet temperature, see Table 2). Therefore, at the valve outlet, when the same enthalpy content is kept, the resulting temperature at 2.5 MPa is higher than the nominal value.

The A.C.1 geometry and RELAP5 results are detailed in Sect. 3.4. Fluid from the four modules is gathered in the condensate tank, operating under saturation conditions, and equipped with an electrical heater to prevent pressure from dropping below 2.5 MPa. Additionally, a safety relief system is placed to prevent overpressures, with a set-point at 3.0 MPa. This results in a wide range of pressure and liquid collapsed levels for the operational point of the condensate tank, depending on the thermodynamic conditions of the fluid from the A.C.1. This variation explains the temperature difference in Table 2. The power supplied by the A.C.2, and consequently the air velocity within it, is contingent on

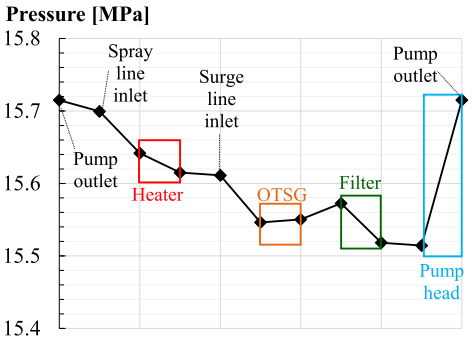

Fig. 7. Pressure profile along the primary loop main components.

the fluid conditions at the A.C.1 outlet. Indeed, a control system manages the A.C.2 air mass flow to achieve a temperature sufficiently below the saturation (210 °C): The A.C.2 power is lower than the reference data, as the fluid already undergoes few degrees of subcooling within the A.C.1 (see Table 2 and discussion in Sect. 3.4). Thanks to the A.C.2 regulation system, the section of the secondary loop from the A.C.2 to the OTSG inlet nozzle remains unaffected by variations in thermodynamic conditions within the STEAM line.

The pump processes the subcooled fluid from the A.C.2 and is expected to deliver a minimum of 40 kW to the fluid (equivalent to nearly a 5 °C temperature increase). However, the model employed in the RELAP5 input deck for this component relies on preliminary homologous curves and design data. Thus, the calculated power provided to the fluid results lower than the nominal value. An update for the pump model is planned as soon as the datasheet of the actual component becomes available during the final design phase. To address this discrepancy, an additional fraction of power is provided by the electric heater (see Table 2), which is regulated by a control system that adjusts its power to achieve 238 °C at the OTSG inlet.

The pressure profiles, tracing the loops main components, are depicted in Figs. 7 and 8 for the primary and secondary loop, respectively. Static descendant column contribution becomes particularly significant, especially in the primary loop, where the absence of STEAM results in higher density. This leads to a pressure increase from the OTSG outlet to the filter inlet, facilitated by the vertical descendant inclination of this section of the loop.

Figs. 9–12 illustrate heat losses and mass inventories for both primary and secondary loops. Heat losses were computed by summing the product of the heat flux and the correspondent surface area of each mesh, considering 10 °C for the environmental temperature and 8 W/m^{2}K for the heat transfer coefficient. Notably, in Figs. 10 and 12, the term "STEAM Line" encompasses not only the 3 ½" piping from the OTSG to the lamination valve but also the following 5″ tube and the four 2″ piping leading to the A.C.1 modules. Most of the primary loop water inventory is concentrated in the pressurizer, while the secondary loop one is concentrated in the condensate. It is worth mentioning that the RELAP5 results for the pump and filter remain preliminary, as these components are yet to be finalized in their design.

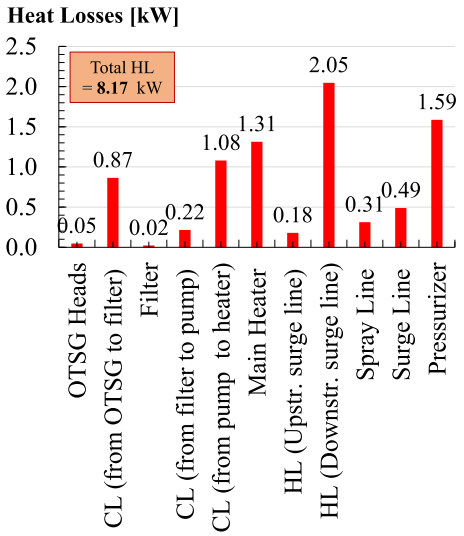

Fig. 9. Primary loop heat losses distribution.

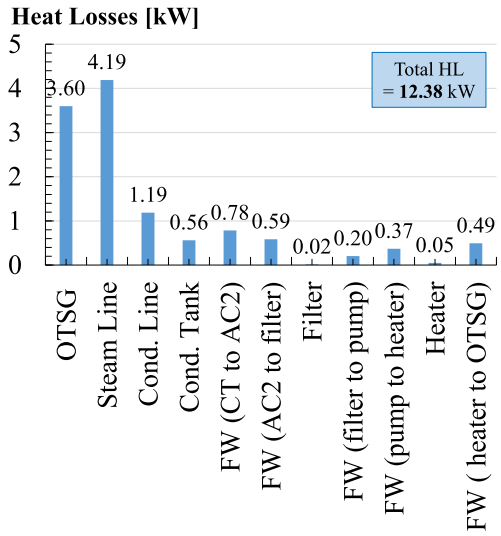

Fig. 10. Secondary loop heat losses distribution.

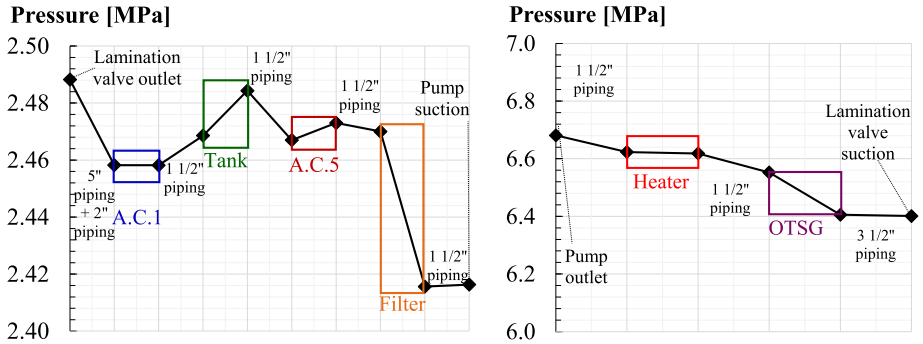

Fig. 8. Pressure profile along the secondary loop from pump outlet to lamination valve inlet (left), from lamination valve outlet to pump suction (right).

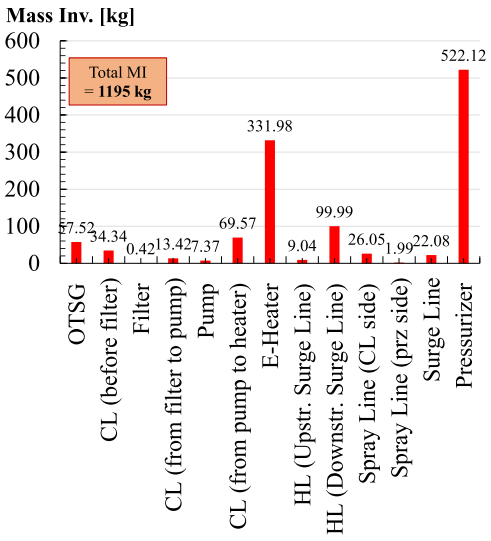

Fig. 11. Primary loop mass inventory distribution.

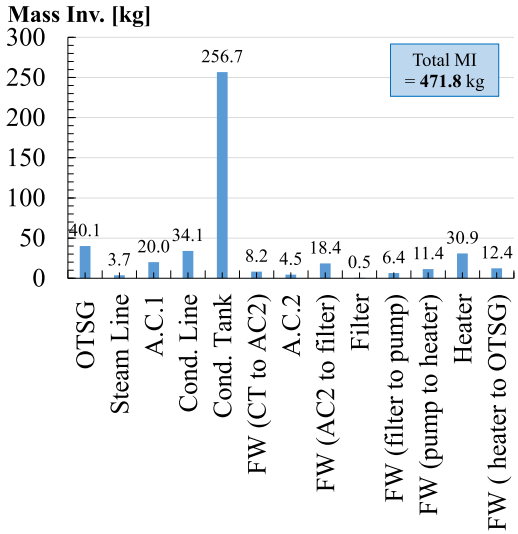

Fig. 12. Secondary loop mass inventory distribution.

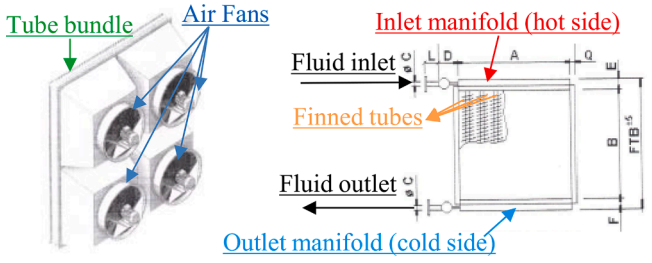

Fig. 13. De-superheating and condensation air cooler module: 3D view (left) and cutaway view of the cooling bundle (right).

3.4. RELAP5 component T/H analysis

The de-superheating and condensation air cooler can be considered a critical component since it mostly operates in saturation conditions. It is composed of four parallel modules characterized by 55 AISI 304 finned tubes organized in a single-passage tube bundle vertically inclined, for a total of 220 tubes each measuring 2.5 m in length. Modules are equipped with four horizontal fans each, from which air in forced convection is perpendicularly headed toward the tube bundle. The sketch of one module is shown in Fig. 13.

Thermal-hydraulic simulations performed with RELAP5/Mod3.3 code on the air cooler components highlighted that conventional control logics are not suitable for adjusting the air mass flow rate. Since they operate under saturation, the outlet temperature is not indicative of the actual fluid thermo-dynamic conditions. Furthermore, air cooler modules experience phase separation as the condensed liquid exhibits a higher heat transfer coefficient compared to the saturated vapor. This leads to significant subcooling of the liquid phase, even when not all the STEAM has condensed. For this reason, the secondary air velocity was set to a value that allows to achieve primary fluid outlet conditions that align as closely as possible with the nominal ones, without inducing excessive subcooling. Results of the analyses conducted on the de-superheating and condensation air cooler are reported in Table 3.

The distribution of the mass flow among the four modules of the A.C.1 directly results from the distinct chain of pressure drops characterizing the lines leading to each module. The small deviations are due to the geometrical asymmetries in the pipe routing. The modules mass flow is linked to the fluid outlet enthalpy, with higher mass flow corresponding to higher enthalpy. However, the different operating pressures of the modules, outlined in Table 3, significantly impact the condensation power of each module, as illustrated in Figs. 14–16.

Further investigations reveal an uneven distribution of mass flow within the tubes of each module. Specifically, it decreases in approaching the further tubes, as depicted in Fig. 17. The exchanged power is a direct outcome of the mass flow and exhibits a similar trend, as shown in Fig. 18.

A measure of the fluid outlet thermo-dynamic conditions is the thermodynamic quality, denoted by values ranging between 0 and 1 for saturation conditions, values >1 for superheated conditions, and <0 for sub-cooling conditions. The air mass flow is constant and uniform for all the modules, whereas vapor mass flow varies in each tube of every module. A decrease in vapor mass flow aligns with a reduction in tube outlet enthalpy, leading to increased sub-cooling (as depicted in Fig. 19) and a greater liquid collapsed level within the tube (as outlined in Table 4).

4. Conclusions

This paper presents the main outcomes of the design phase of STEAM innovative experimental facility, which is planned for construction at the ENEA Brasimone Research Centre. The facility is designed with the primary objective of experimentally characterizing and validate the DEMO WCLL BoP water coolant systems encompassing steady-state tests as well as operational transients, including pulse-dwell-pulse scenarios. A specific focus is on demonstrating the SG capability to follow rapid load variations as well as to operate at very low constant power levels.

In pursuit of this goal, STEAM facility will host a 1:1-scaled-in-length mock-up of the DEMO BB SG. In addition, the experimental setup will be equipped with two thermally independent loops that will reproduce the thermodynamic conditions of the DEMO BB PHTS (15.5 MPa, 328–295 °C) and Power Conversion System (PCS, 6.4 MPa, 238–300 °C). Results of the experimental campaigns will play a crucial role in the pathway toward nuclear fusion energy production, providing fundamental data for the characterization and validation of components within a fusion environment. In particular, the scaling process adopted to design the layout of the OTSG in the STEAM facility should ensure the extendibility of STEAM results to the STEAM generators of DEMO, facilitating the characterization of primary phenomena, flow regimes, and heat exchange regimes.

The thermal-hydraulic reproduction of the whole facility was performed using RELAP5/Mod3.3 code to assess the stability and compliance of the main parameters with their nominal values. The scaling of the SG test section at BoL conditions determined some deviations from

Table 3
De-superheating and condensation air cooler RELAP5 results.

Parameter	Unit	Module #				R5 Total/Avg	Des.	Er.
		Module 1	Module 2	Module 3	Module 4			
$p_{A.C.1}$	Mpa	2.458	2.461	2.460	2.458	2.459	2.5	−1.6 %
$T_{downstream\ A.C.1}$	°C	220.1	223.1	223.1	202.5	217.2	224.0	−6.8 °C
$VF^{a}_{upstream\ A.C.1}$	-	1.00	1.00	1.00	1.00	1.00	1.00	0.0%
$VF^{a}_{downstream\ A.C.1}$	-	0.00	0.04	0.03	0.00	0.02	0.00	+2%
$h_{downstream\ A.C.1}$	kJ/kg	944.0	959.0	958.7	863.7	931.4	962.0	−3.2 %
Power	MW	0.81	0.81	0.81	0.81	3.25	3.108	+4.6 %
$T_{upstream\ C.T.}$	°C	220.8				217.3	224	−6.67 °C

[a] VF stands for void fraction.

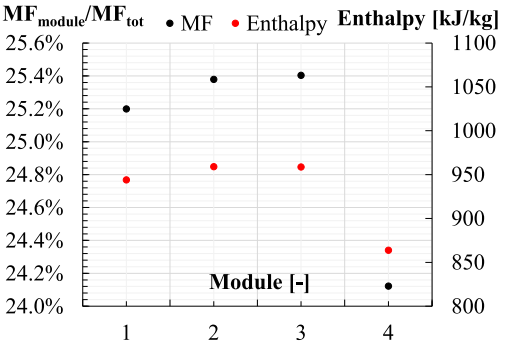

Fig. 14. A.C.1 mass flow distribution among the modules and fluid outlet enthalpy.

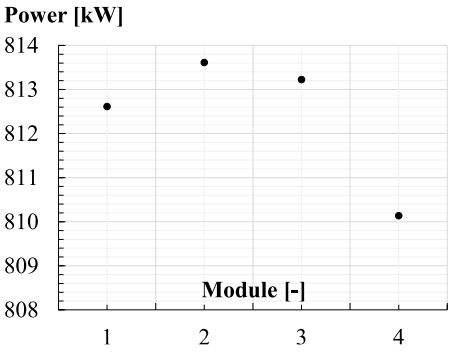

Fig. 15. A.C.1 modules exchanged power.

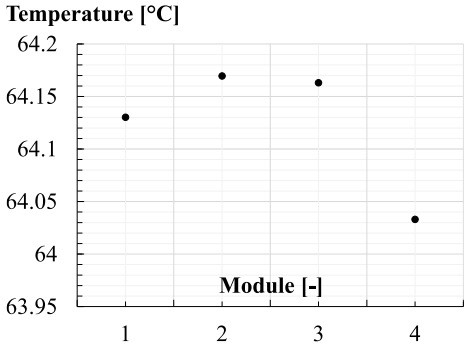

Fig. 16. A.C.1 modules air outlet temperature.

the nominal parameters (i.e., STEAM outlet temperature). The conducted analyses highlighted that such deviations are localized to the section of the secondary loop between the test section outlet and the A.

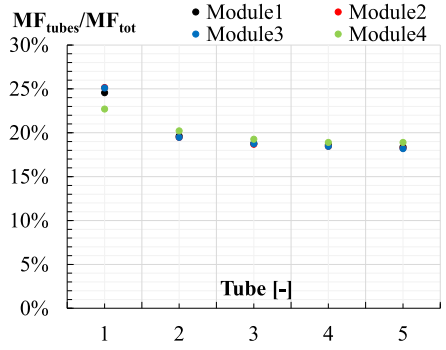

Fig. 17. A.C.1 mass flow distribution.

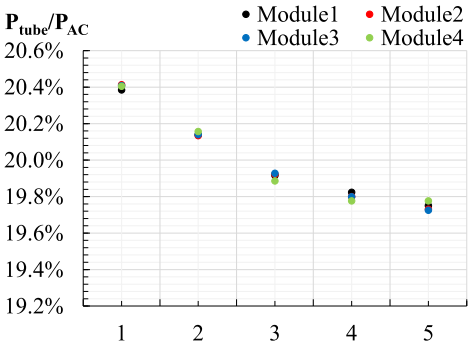

Fig. 18. A.C.1 power distribution.

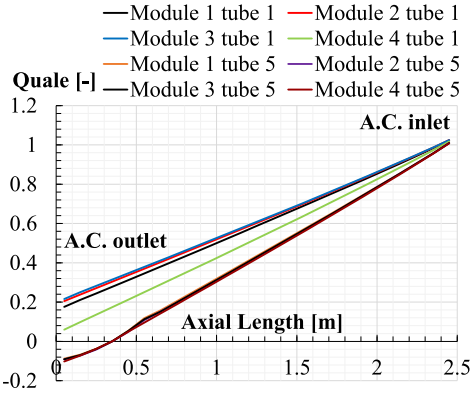

Fig. 19. A.C.1 equilibrium quality (Quale) axial profile along the first and the last tube of each module.

Table 4
A.C.1 liquid collapsed level of the first and the last tube of each module.

Parameter	Unit	Value
Module 1 tube 1	m	0.026
Module 1 tube 5	m	0.372
Module 2 tube 1	m	0.027
Module 2 tube 5	m	0.366
Module 3 tube 1	m	0.027
Module 3 tube 5	m	0.366
Module 4 tube 1	m	0.026
Module 4 tube 5	m	0.384

C.1 outlet. However, these differences do not diminish the representativeness of the test section. Focus was also directed towards the evaluation of the performances of the de-superheating and condensation Air Cooler. Given their critical operation in saturation conditions, it is fundamental to characterize their T/H behavior to provide valuable feedbacks on the regulation strategy to be adopted. To avoid phase separation inside the A.C.1 modules determining excessive subcooling of the fluid, air mass flow influence on the component performances was assessed and its value was adjusted to achieve primary fluid outlet conditions closely aligned with nominal ones. Geometrical asymmetries in the realization of the four pipes affect their operation in parallel, due to the uneven distribution of the mass flow rates among the modules, resulting in different power removals and fluid outlet conditions. Therefore, air cooler performances are evaluated based on the thermodynamic conditions of the water after the mixing of the four branches.

CRediT authorship contribution statement

Alessandra Vannoni: Writing – review & editing, Writing – original draft, Visualization, Validation, Software, Methodology, Investigation, Formal analysis, Data curation, Conceptualization. **Pierdomenico Lorusso:** Writing – review & editing, Validation, Supervision, Software, Methodology, Investigation, Formal analysis, Data curation, Conceptualization. **Marica Eboli:** Writing – review & editing, Validation, Supervision, Resources, Project administration, Methodology, Investigation, Funding acquisition, Conceptualization. **Fabio Giannetti:** Writing – review & editing, Validation, Supervision, Resources, Investigation, Formal analysis, Data curation, Conceptualization. **Cristiano Ciurluini:** Writing – review & editing, Validation, Supervision, Software, Methodology, Investigation, Formal analysis, Data curation, Conceptualization. **Diego Jaramillo Sierra:** Writing – review & editing, Visualization, Software, Methodology, Investigation, Data curation, Conceptualization. **Alessandro Del Nevo:** Writing – review & editing, Validation, Supervision, Software, Resources, Methodology, Investigation, Formal analysis, Conceptualization.

Declaration of competing interest

The authors declare that they have no known competing financial interests or personal relationships that could have appeared to influence the work reported in this paper.

Data availability

Data will be made available on request.

Acknowledgments

This work was carried out within the framework of the EUROfusion Consortium, funded by the European Union via the Euratom Research and Training Programme (Grant Agreement No 101052200 — EUROfusion). Views and opinions expressed are however those of the author (s) only and do not necessarily reflect those of the European Union or the European Commission. Neither the European Union nor the European Commission can be held responsible for them.

References

[1] G. Federici, et al., An overview of the EU breeding blanket design strategy as an integral part of the DEMO design effort, Fusion Eng. Des. 141 (2019) 30–42, https://doi.org/10.1016/j.fusengdes.2019.01.141. April 2019, Pages.
[2] L.V. Boccaccini, F. Arbeiter, P. Arena, J. Aubert, L. Buhler, I. Cristescu, A. Del Nevo, M. Emboli, L. Forest, C. Harrington, et al., Status of maturation of critical technologies and systems design: breeding blanket, Fusion Eng. Des. 179 (2022) 113116, https://doi.org/10.1016/j.fusengdes.2022.113116.
[3] G. Federici, et al., An overview of the EU breeding blanket design strategy as an integral part of the DEMO design effort, Fusion Eng. Des. 141 (2019) 30–42, https://doi.org/10.1016/j.fusengdes.2019.01.141.
[4] V.P. Muratov, et al., ITER – international thermonuclear experimental reactor, fundamentals of magnetic thermonuclear reactor design, Woodhead Publ. Ser. Energy (2018) 39–67, https://doi.org/10.1016/B978-0-08-102470-6.00003-2.
[5] L.M. Giancarli, et al., Overview of recent ITER TBM program activities, Fus. Eng. Des. 158 (2020) 111674, https://doi.org/10.1016/j.fusengdes.2020.111674.
[6] C. Ciurluini, et al., Conceptual design overview of the ITER WCLL Water Cooling System and supporting thermal-hydraulic analysis, Fusion Eng. Des. 171 (2021) 112598, https://doi.org/10.1016/j.fusengdes.2021.112598.
[7] K. Jiang, et al., Thermal-hydraulic analysis on the whole module of water cooled ceramic breeder blanket for CFETR, Fusion Eng. Des. 112 (2016) 81–88, https://doi.org/10.1016/j.fusengdes.2016.07.027.
[8] X. Cheng, et al., Primary heat transfer system design of the WCCB blanket for multiple operation modes of CFETR, Fusion Eng. Des. 153 (2020) 111489, https://doi.org/10.1016/j.fusengdes.2020.111489.
[9] G.S. Lee, et al., Design and construction of the KSTAR tokamak, Nucl. Fusion 41 (10) (2001) 1515–1523, https://doi.org/10.1088/0029-5515/41/10/318. Issue.
[10] J.G. Kwak, et al., Key features in the operation of KSTAR, Proceedings - Symposium on Fusion Engineering (2011), Chicago, Illinois, USA 26 – 30, 2011, doi:10.1109/SOFE.2011.6052198.
[11] (2024) https://www.euro-fusion.org/.
[12] M. Tarantino, et al., Fusion technologies development at ENEA brasimone research centre: status and perspectives, Fusion Eng. Des. 160 (2020) 112008, https://doi.org/10.1016/j.fusengdes.2020.112008.
[13] A. Vannoni, et al., The design of water loop facility for supporting the WCLL breeding blanket technology and safety, Energies 16 (2023) 7746, https://doi.org/10.3390/en16237746 (Basel).
[14] N. Badodi, et al., Status, features, and future development of the LIFUS5/Mod4 experimental facility design, Appl. Sci. 13 (2023) 482, https://doi.org/10.3390/app13010482.
[15] S. Ciattaglia, et al., EU DEMO safety and balance of plant design and operating requirements. Issues and possible solutions, Fusion Eng. Des. 146 (2019) 2184–2188, https://doi.org/10.1016/j.fusengdes.2019.03.149. Part B, September 2019, Pages.
[16] A. Vannoni, et al., STEAM experimental facility: a step forward for the development of the EU DEMO BoP water coolant technology, Energies 16 (2023) 7811, https://doi.org/10.3390/en16237811 (Basel).
[17] A. Vannoni, et al., The STEAM facility: design and analysis, in: Proceedings of the NURETH20, Washington DC (USA), 2023, https://doi.org/10.13182/NURETH20-40567. August 20-25.
[18] A. Tincani, Conceptual design of the steam generators for the EU DEMO WCLL reactor, Energies 16 (2023) 2601, https://doi.org/10.3390/en16062601 (Basel).
[19] A. Del Nevo, et al., Recent progress in developing a feasible and integrated conceptual design of the WCLL BB in EUROfusion project, Fusion Eng. Des. 146 (2019) 1805–1809, https://doi.org/10.1016/j.fusengdes.2019.03.040.
[20] A. Vannoni, A. Development of a steam generator mock-up for EU DEMO fusion reactor: conceptual design and code assessment, Energies 16 (2023) 3729, https://doi.org/10.3390/en16093729 (Basel).
[21] L. Barucca, et al., Maturation of critical technologies for the DEMO balance of plant systems, Fusion Eng. Des. 179 (2022) 113096, https://doi.org/10.1016/j.fusengdes.2022.113096.
[22] I. Moscato, et al., Tokamak cooling systems and power conversion system options, Fusion Eng. Des. 178 (2022) 113093, https://doi.org/10.1016/j.fusengdes.2022.113093.
[23] I.S.L. Inc, RELAP5/Mod3.3 code manual volume I: code structure, system models, and solution methods, Nucl. Saf. Anal. Div. (2003). July.
[24] A. Vannoni, et al., RELAP5/Mod3.3 thermal-hydraulics characterization of the steam generator mock-up during operational transients in STEAM facility in support of the design of the DEMO WCLL BoP, Fusion Eng. Des. 200 (2024) 114165, https://doi.org/10.1016/j.fusengdes.2024.114165.
[25] L. Barucca, et al., Pre-conceptual design of EU DEMO balance of plant systems: objectives and challenges, Fusion Eng. Des. 169 (2021) 112504, https://doi.org/10.1016/j.fusengdes.2021.112504.
[26] G. Federici, et al., DEMO design activity in europe: progress and updates, Fusion Eng. Des. 136 (2018) 729–741, https://doi.org/10.1016/j.fusengdes.2018.04.001.
[27] L. Barucca, et al., Status of EU DEMO heat transport and power conversion systems, Fusion Eng. Des. 136 (2018) 1557–1566, https://doi.org/10.1016/j.fusengdes.2018.05.057.
[28] A. Collaku, et al., Design of a test section for the experimental investigation of the WCLL manifold hydraulic features, Energies 16 (5) (2023), https://doi.org/10.3390/en16052246 (Basel).

[29] C. Ciurluini, et al., Thermal-hydraulic assessment of once-through steam generators for EU-DEMO WCLL breeding blanket primary cooling system application, Fusion Eng. Des. 193 (2023) 113688, https://doi.org/10.1016/j.fusengdes.2023.113688.
[30] The US Nuclear Regulatory Commission (USNRC), RELAP5/MOD3.3 Code Manual Volume 4, Models and Correlations, NUREG/CR-5535; USNRC, The US Nuclear Regulatory Commission (USNRC), 2006.
[31] F.W. Dittus, L.M.K. Boelter, Heat transfer in automobile radiators of the tubular type. Publications in Engineering 2, University of California, Berkeley, 1930, pp. 443–461.
[32] A.Y. Inayatov, Correlation of data on heat transfer flow parallel to tube bundles at relative tube pitches of $1.1 < s/d < 1.6$, Heat Transf. Sov. Res. 7 (3) (1975) 84–88. May-June.
[33] J.C. Chen, A correlation for boiling heat transfer to saturated fluids in convective flow, Process Des. Dev. 5 (1966) 322–327.
[34] D.C. Groeneveld, AECL-UO critical heat flux lookup table, Heat Transf. Eng. 7 (1–2) (1986) 46–62, 1986.
[35] J.C. Chen, R.K. Sundaram, A phenomenological correlation for post-CHF heat transfer. NUREG-0237, 1977.
[36] L.A. Bromley, Heat Transfer in Stable Film Boiling, Chem. Eng. Prog. 46 (1950) 221–227.
[37] Y. Sudo, Film boiling heat transfer during reflood phase in postulated PWR loss-of-coolant accident, J. Nucl. Sci. Technol. 17 (7) (1980) 516–530.
[38] W. Nusselt, Die oberflachenkondensation des wasserdampfes, Ver. deutsch. Ing. 60 (1916).
[39] M.M. Shah, A general correlation for heat transfer during film condensation inside pipes, Int. J. Heat Mass Transf. 22 (1979) 547–556.
[40] M.M. Shah, Heat Transfer and Fluid Flow Data Books, Genium Publishing, 1992. JanuarySec. 507.6 p. 8.